1 **Long-term stability of dithionite in alkaline anaerobic aqueous solution**

2 Katherine Telfeyan[*], Artas A. Migdisov, Sachin Pandey, Velimir V. Vesselinov, and Paul W.
3 Reimus
4

5 *Earth and Environmental Sciences Division, Los Alamos National Laboratory, Los Alamos, NM*
6 *87545, United States*
7

8 *Corresponding author: Phone: +1 505 665 3880; e-mail: ktelfeyan@lanl.gov

9 **Abstract**

10   Closed-system experiments were conducted to investigate the decomposition of sodium
11 dithionite in aqueous solutions under varying pH and starting concentrations to simulate the
12 deployment of dithionite as an in-situ redox barrier. Co-determination of dithionite and its
13 degradation products was conducted using UV-Vis spectrometry, iodometric titration, and ion
14 chromatography. In unbuffered solutions, dithionite reacted rapidly, whereas in near-neutral
15 solutions (pH ~7), it persisted for ~ 50 days and in alkaline solution (pH ~9.5) for >100 days.
16 These are the longest lifetimes reported to date, which we attribute to not only excluding oxygen
17 but also preventing outgassing of H_2S. Thoroughly constraining the reaction products has led to
18 the following hypothesized reaction:

19    $4\ S_2O_4^{2-} + H_2O \rightarrow HS^- + SO_3^{2-} + 2\ SO_4^{2-} + S_4O_6^{2-} + H^+$

20 which represents relatively rapid degradation at near-neutral pH values. At the more alkaline pH,
21 and over longer time scales, the reaction is best represented by:

22    $3\ S_2O_4^{2-} + 3\ H_2O \rightarrow 2HS^- + SO_3^{2-} + 3\ SO_4^{2-} + 4\ H^+$

23 the following kinetic rate law was developed for the pH range studied:

$$\frac{dC_i}{dt} = S_i 10^{-4.81}\{H^+\}^{0.24}\{S_2O_4^{2-}\},$$

24 where $\frac{dC_i}{dt}$ is the rate of change of the ith chemical component in the simplified equation (mole L^{-1}
25 s^{-1}) and S_i is the stoichiometric coefficient of the ith chemical. The kinetic rate law was used to
26 calculate a pseudo first order half-life of 10.7 days for near-neutral pH and 33.6 days for alkaline
27 pH. This work implies that if hydrogen sulfide is contained within the system, such as in the case
28 of a confined aquifer below the water table, dithionite decomposes more slowly in alkaline
29 aqueous solution than previously thought, and thus it may be more cost-effectively distributed in
30 aquifers than has been previously assumed.

31 **Keywords:** dithionite; sulfur redox chemistry; hydrolysis reaction; in-situ redox manipulation

32

33

34

35

I.   Introduction

36   **I.   Introduction**

37   Sulfur is among the most important elements controlling redox equilibria in natural

38   aqueous systems, including high temperature sub-magmatic fluids, geothermal waters, acid-

39   sulfate pools, as well as low temperature systems such as wetlands and geochemical systems

40   artificially created in subsurface aquifers during remediation of contaminated horizons (Luther

41   and Church, 1988; Migdisov and Bychkov, 1998; Fruchter et al., 2000; Burton et al., 2011;

42   Kassalainen and Stefánsson, 2011a,b; Couture et al., 2016). Complexity of the response of sulfur

43   equilibria to changing redox conditions and, thus, its ability to fine-tune redox conditions of

44   geochemical systems, is due to a large number of oxidation states and intermediate species that

45   this element can form in aqueous solutions. The transfer of 8 electrons during oxidation of

46   sulfide to sulfate produces species such as, SO_3^{2-}, $S_2O_3^{2-}$, S_8°, polysulfides, and polythionates,

47   with the relative proportions depending upon the oxidation state and pH of the system

48   (Kassalainen and Stefánsson, 2011a,b). Quantitative understanding of their relationships is

49   therefore crucial for constraining geochemical controls of these systems and predicting

50   geochemical behavior of redox-sensitive elements. Considerable work has focused on

51   characterizing the S speciation in environments such as hydrothermal waters (Xu et al., 1998;

52   Kassalainen and Stefánsson, 2011a,b), and crater lakes (Casas et al., 2016; Takano, 1987;

53   Takano and Watanuki, 1990; Takano et al., 1994a,b). Changes in sulfur species distribution have

54   also been used as a tool for monitoring volcanic activity and fault geometry (Casas et al., 2016;

55   Takano, 1987; Takano and Watanuki, 1990; Takano et al., 1994a,b). Many of these intermediate

56   redox species, however, are metastable, and thus their distribution depends largely on kinetics,

57 making accurate quantitative determination difficult (Kassalainen and Stefánsson, 2011a,b;

58 Williamson and Rimstidt, 1992).

59   From the point of view of environmental geochemistry, a particularly important

60 intermediate, sodium dithionite, has proven invaluable in environmental remediation for in-situ

61 redox treatment of contaminated groundwater as a strong reducing agent (Istok et al., 1999;

62 Amonette et al., 1994). Dithionite reduces structural ferric iron in iron-bearing minerals

63 according to

64      $S_2O_4^{2-} + 2Fe(III)_{(s)} + 2H_2O \rightarrow 2SO_3^{2-} + 2Fe(II)_{(s)} + 4H^+$ (1)
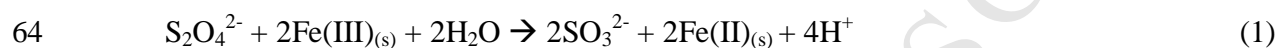
65 forming a permeable treatment zone, capable of reducing and immobilizing certain redox-

66 sensitive elements (Istok et al., 1999). Dithionite has been successfully used to treat plumes of

67 Cr(VI) (Istok et al., 1999; Fruchter et al., 2000; Amonette et al., 1994; Ludwig et al., 2007),

68 perchloroethylene (Nzengung et al., 2001), trichloroethylene (Szecsody et al., 2004), and

69 explosive contaminants (Boparai et al., 2008). Additionally, dithionite has been shown to extend

70 the lifetime of nanoscale zero-valent iron also used in contaminant removal (Xie and Cwiertny,

71 2010). Yet, dithionite is unstable, and the concentration of dithionite itself and its degradation

72 products changes with time and is highly dependent on the aquifer conditions (Holman and

73 Bennett, 1994). Geochemical modelling of the systems on which this remediant has been applied

74 and evaluation of the longevity of its effects therefore require quantitative knowledge of its

75 degradation rate, stoichiometry of its decomposition, and variability of these properties with

76 changing aquifer conditions.

77   Unfortunately, the data currently available in the literature on the lifetime of dithionite

78 and its decomposition products are highly scattered (Table 1). One of the factors influencing

79 determined decomposition rates of dithionite and, thus, partially explaining scattering of the data,

3

80   is the pH at which experiments were performed. It has been consistently shown since the initial

81   work in the early 1900s that decomposition of dithionite greatly accelerates when pH decreases.

82   The greater decomposition under acidic conditions is attributed to a greater decomposition rate

83   of the protonated species $HS_2O_4^-$ or $H_2S_2O_4$ relative to the unprotonated $S_2O_4^{2-}$, which is

84   predominant in alkaline solutions (Lister and Garvie, 1959). Therefore, dithionite in unbuffered

85   or acidic solution is impractical as a treatment option, and all previous deployments have added a

86   basic buffer to extend its lifetime. For example, during deployment of dithionite to treat a Cr(VI)

87   plume, Istok et al. (1999) buffered the dithionite solution with a CO_3^{2-}/HCO_3^- solution to pH ~11.

88   Dithionite decomposition is slower in anaerobic, alkaline solutions and reportedly follows

89   pseudo-first order decay (Ammonette et al., 1994; Lister and Garvie, 1959) or half-order decay

90   in excess alkali (Kilroy, 1980). However, even in alkaline solution, the data on dithionite

91   decomposition is inconsistent (Table 1). Previously reported experimental rate constants vary

92   from $4.5 \cdot 10^{-4}$ min^{-1} (88.5^{o}C) (Lister and Garvie, 1959), 0.015 M$^{0.5}$min^{-1} (82°C) (Kilroy, 1980),

93   and 4.8-$8.5 \cdot 10^{-5}$ min^{-1} (varying dithionite concentrations; Amonette et al., 1994). At pH 13,

94   Münchow and Steudel (1994) observed no noticeable loss of dithionite from anaerobic solution

95   for the duration of their study (4 days), but Amonette et al. (1994) measured dithionite after ~ 2

96   weeks. One explanation for such discrepancies is the extent of containment of the experimental

97   solutions. Indeed, if the suggestion of the formation of H_2S as the decomposition product of

98   dithionite is correct (Wayman and Lem, 1970), poor containment of the system should inevitably

99   lead to losses of this component from the solution and acceleration of the decomposition of

100   dithionite. These losses can potentially occur as degassing of the solution due to formation of

101   H_2S gas (even in inert gas-filled compartments, such as gloveboxes), or, if solutions are not

102   protected from the atmosphere, due to oxidation of H_2S by atmospheric oxygen. It should be

4

103 noted that the majority of the experimental studies referred to above prevented oxygen intrusion

104 but did not take any special precaution to address the outgassing of H_2S, and therefore they may

105 have underestimated the dithionite lifetimes. Moreover, the vast majority of the studies available

106 in the literature on the decomposition of dithionite have been performed for durations not

107 exceeding 2 weeks, primarily due to quick decomposition of dithionite. However, if this quick

108 decomposition is caused by the effects discussed above (e.g., poor containment of the solutions),

109 these data can be misleading for modeling dithionite behavior in anoxic aquifers in which

110 confined conditions with respect to gas exchange often exist and in which the lifetime of

111 dithionite can potentially be significantly longer. Even in oxic aquifers, anoxic conditions will

112 eventually prevail in the immediate vicinity of an injection well because the injected dithionite

113 will consume all available oxidants near the well. If dithionite is continuously injected under

114 these conditions, the distance that it can ultimately be pushed into an aquifer will be dictated by

115 its anaerobic decomposition rate in the presence of aqueous phase reaction products. The goal of

116 our study is therefore to investigate the stability of dithionite in well-contained systems and, if it

117 is found that containment increases the life time of dithionite, to expand the time range up to

118 months. This study also offers a working model that incorporates the important effect of pH on

119 dithionite degradation rates in anoxic systems. Although other research to support field

120 deployments has noted the effect of pH on dithionite lifetime, they have not incorporated this

121 effect into a rate law to accurately predict dithionite degradation through time.

122

123 Table 1. Summary of previous studies' experimental conditions and results.

Reference	Experimental Conditions	Results
Lister and Garvie (1959)	$T=88^{o}C$; N_2 atmosphere; $[S_2O_4^{2-}]$= 0.034-0.142 M; Buffer: 0.05-0.2 M NaOH	$k=4.5 \cdot 10^{-4}$ min^{-1}
Rinker et al.	$T=60-80^{o}C$;	$R_{induction}=k_c[S_2O_4^{2-}]r^{3/2} \cdot [H^+]^{1/2}$

(1965)	$[S_2O_4^{2-}]$= 0.0055-0.0115 M; pH=4-7 (KH$_2$PO$_4$ and NaOH)	k_c=1.3·10^8·e^{-12000}/RT L mol^{-1} sec^{-1}
Spencer (1967)	T=15-35°C $[S_2O_4^{2-}]$= 0.015-0.2 M in solution of HSO$_3^-$, SO$_3^{2-}$, NaCl (pH 5.2)	First-order decay Decomposition products: trithionate, thiosulfate
Burlamacchi et al. (1969)	T=60-90°C $[S_2O_4^{2-}]$= 0.067, 0.125, 0.25 M; pH=6 (phosphate buffer)	-d[S2O42-]/dt = k'[S2O42-][HSO3-] k'=0.57-7.8·10^3 L mole^{-1} s^{-1}
Lem and Wayman (1970)	T=23°C; Ar atmosphere; $[S_2O_4^{2-}]$=1, 2, 5, 10·10^{-3} M; pH range: 3.5, 4, 4.5, 5 (Buffers: acetate, sodium hydrogen phosphate-citric acid)	-dC/dt=k$_1$[H$^+$]C + k$_2$[H$^+$]C(C^o-C) k$_1$: 1.67·10^{-1} L mol^{-1}s^{-1} k$_2$=5.83·10^3 L^2 mole^{-2} s^{-1}
Kilroy (1980)	T=82°C; Ar atmosphere; $[S_2O_4^{2-}]$=0.02-0.08 M; Buffer: NaOH	k=0.014-0.018 (mol/L)$^{-0.5}$ min^{-1}
Holman and Bennett (1994)	T=42-88.5^{o}C; N$_2$ purged Excess Bisulfite pH: mildly acidic	d$[S_2O_4^{2-}]$/dt= -k$_1$$[S_2O_4^{2-}]$[HSO$_3^-$]-k$_2$$[S_2O_4^{2-}]^{0.5}$[HSO$_3^-$][S$_3O_6^{2-}$] k$_1$=(3.1±0.3·10^2 M^{-1} s^{-1}·T·exp(-(54.3±5)/RT) k$_2$=(1.67±0.2·10^7 M$^{-3/2}$ s^{-1}·T·exp(-(78.4±7)/RT)
Münchow and Steudel (1994)	T=20°C; $[S_2O_4^{2-}]$=0.0214 M; pH: 5.7, 13	Reaction products: thiosulfate, sulfite Dithionite in alkaline solution persists (Experiments not exceeding 2 hours)
Amonette et al. (1994)	T=30°C; Ar (95%), H$_2$(4%); $[S_2O_4^{2-}]$=0.002, 0.013, 0.06 M; CaCO$_3$ buffer	0.06 M: t$_{1/2}$=135 h; k$_{app}$=8.5·10^{-5} min^{-1} 0.002 M: t$_{1/2}$=243 h; k$_{app}$=4.8·10^{-5} min^{-1}
de Carvalho and Schwedt (2001)	$[S_2O_4^{2-}]$=0.0065 M Background solutions of formaldehyde, NaOH, HMTA in glyceral and water, diammonium hydrogen phosphate/ammonium hydroxide, Triton X-100	Major reaction products: sulfite thiosulfate Minor reaction products: sulfide, elemental S

124

125

II. Materials and Methods

II.A. Sample Preparation

Experiments involved determination of the concentrations of dithionite and its decomposition

products in solutions contained in sealed 10 ml glass ampoules. Considering that the typical pH

observed in the solutions of treated aquifers ranges from 7 to 10, experiments were performed in

three types of solutions: 1) 0.1 M sodium bicarbonate (Certified ACS, Fisher scientific; pH =

7.8-8.3), hereafter referred to as the HCO$_3^-$ buffered solutions, 2) 1 wt%

6

133   ethylenediaminetetraacetic acid, disodium salt dehydrate, 0.6 wt% potassium carbonate, 0.5 wt%

134   potassium hydroxide, and 0.4 wt% potassium borate (pH = 9.8 – 10; Fisher Scientific pH 10

135   buffer solution), hereafter referred to as the EDTA/OH⁻ buffered solutions, and 3) in pH-

136   unbuffered deionized water. Dithionite solutions were prepared by dissolving $Na_2S_2O_4$

137   (Laboratory Grade, Fisher Scientific) in the above solutions. Experiments were performed at

138   room temperature ($25^{o}C$) with solutions having three initial concentrations of dithionite, 0.1 M,

139   0.05 M, 0.025 M, which were chosen to encompass the range of concentrations used in previous

140   field injections (Istok et al., 1999; Fruchter et al., 2000). Prior to addition of dithionite salt, all

141   solutions were degassed under vacuum and thereafter intensively purged with Ar gas to remove

142   any traces of oxygen. Solutions were transferred via syringe into Ar-purged glass ampules. The

143   ampules were immediately flame sealed to prevent oxygen intrusion into the solutions and

144   potential losses of H_2S out of them. A cloudy appearance was observed in the unbuffered 0.05 M

145   and 0.025 M solutions, which disappeared in less than one day. All glass ampules used in the

146   study were filled the same day (total of 108 ampoules) and left undisturbed until sampled.

147   Sampling of the solutions was performed after 1, 3, 7, 10, 14, 29, 45, 55, 66, 78, 86, and 105

148   days from the beginning of the experiment. Each sampling involved opening of 9 ampoules (0.1

149   M, 0.05 M, 0.025 M / HCO_3^- buffered solutions, EDTA/OH⁻ buffered solutions, unbuffered) and

150   determination of S species and pH. Sampling was performed immediately after opening the

151   ampoule, and analyses for all analytes were conducted as quickly as possible (approximately 5

152   min.).

153   *II.B. Sample Analyses*

154   For each sampling event, solutions were analyzed for concentrations of dithionite,

155   sulfide, sulfite, thiosulfate, and sulfate. We also determined pH and, to control the mass balance

7

156 of sulfur, total concentration of sulfur species able to interact with iodine (dithionite, sulfide,

157 sulfite, thiosulfate, and polythionates, except $S_2O_6^{2-}$).

158   *II.B.i. UV-Vis analysis: $S_2O_4^{2-}$, SO_3^{2-}*

159   When a vial was broken for sampling, an aliquot was immediately taken for UV-vis

160 analysis (dithionite, sulfite, and thiosulfate) on a Shimadzu UV-2600 spectrophotometer. UV-vis

161 spectra of experimental solutions were recorded in a flow-through cuvette under strictly oxygen-

162 free conditions for the wavelengths ranging from 190 to 400 nm with an increment of 1 nm. A

163 glass vial, containing 50 mL distilled water and 1 mL of 0.1 M HCO_3^-, which was continuously

164 purged with Ar, was connected with tygon tubing to the cuvette. Continuous circulation of the

165 solution between the vial and the cuvette was forced by peristaltic pump.

166   Dithionite concentrations were measured at a wavelength of 350 nm (Ammonette et al.,

167 1994). Sulfite was determined at a wavelength of 200 nm. Although the $S_2O_3^{2-}$ and SO_3^{2-} UV-vis

168 spectra overlap, both deconvolution of the UV-vis spectra and titration with formaldehyde

169 described below indicated negligible thiosulfate formation. Owing to the near-immediate partial

170 degradation of dithionite, calibrating the UV-vis spectral signal of dithionite-bearing solutions is

171 essential, yet non-trivial. Known amounts of dithionite salt were added to glass vials pre-purged

172 with Ar gas and sealed with rubber stoppers. The buffer solutions were then added by syringe

173 through the rubber stoppers. Upon complete dissolution of the salt, an aliquot was extracted by

174 syringe and UV-vis spectra were recorded. Another aliquot was taken for iodometric titration to

175 determine dissolved sulfur species as described below. The latter indicated that ~50% of the

176 dithionite underwent immediate decomposition

177   *II.B.ii. Iodimetric Titration*

178   Another aliquot of sample was taken for iodometric titration, which determines total

179   reduced sulfur species (Danehy and Zubritsky, 1974; Szekeres, 1974; Migdisov and Bychkov,

180   1998). This technique was used to determine a mass balance as it measures the concentration of

181   all S species except oxidized S (i.e., SO_4^{2-}), elemental S, and $S_2O_6^{2-}$. In some selected samples,

182    $S_2O_3^{2-}$ was also determined through iodometric titration with formaldehyde (Danehy and

183   Zubritsky, 1974; Szekeres, 1974), but these analyses determined that thiosulfate formation was

184   negligible.

185   The concentrations of dissolved sulfide sulfur (H_2S, HS^-) in the solutions were

186   determined by precipitation with Cd acetate and iodometric back titration. The technique

187   involves precipitation of sulfide sulfur in the form of insoluble CdS (by adding an aliquot of Cd

188   acetate), separation of the precipitate from the solution by centrifuging or filtration, and the

189   aforementioned iodometric back titration of the solid precipitate in an aliquot having an excess of

190   HCl and iodine by sodium thiosulfate (Szekeres, 1974).

191   *II.B.iii Ion Chromatography (SO_4^{2-})*

192   Oxidized S (i.e., SO_4^{2-} analysis) was determined on a Dionex ICS-2100 Ion

193   Chromatography System. The aliquots which were not analyzed immediately after sampling,

194   were immediately frozen to stop decomposition of dithionite and preclude continuous

195   accumulation of decomposition products.

196   Any S in excess of the independently determined $S_2O_4^{2-}$, SO_3^{2-}, HS^-, SO_4^{2-} and $S_2O_3^{2-}$ can

197   be attributed to zero valent sulfur, some of the polythionate species, and/or elemental sulfur

198   involved in polysulfane chains.

199   *II.C. Kinetics of dithionite decomposition*

9

200   A numerical model was formulated to quantify the kinetics of dithionite degradation in the

201   HCO_3^- and EDTA/OH^- buffered experiments. The unbuffered experiments were not modeled

202   because degradation was so rapid that it was considered impractical to consider using dithionite

203   without buffering. No attempt was made to model the very rapid initial degradation of

204   dithionite. To allow for quantitative comparison of the HCO_3^- and EDTA/OH^- buffered

205   experiments, a kinetic model was developed based upon the experimentally deduced

206   stoichiometry (Equation (4) in Section IVA) for both sets of experiments. The kinetic rate

207   expression assumed first order dependence on dithionite concentration and a fractional order

208   dependence on proton activity:

209    $$\frac{dC_i}{dt} = S_i k \{H^+\}^{\propto} \{S_2O_4^{2-}\}, \qquad (2)$$

210   where C_i is the concentration at each time step and S_i is the stoichiometric coefficient of the ith

211   chemical component in Equation (4), t is time (s), k is the kinetic rate constant, $\propto$ is a fractional

212   exponent, and $\{S_2O_4^{2-}\}$ and $\{H^+\}$ are the respective dithionite and proton activities at each time

213   step. The inclusion of a fractional order dependence on proton activity reflects an autocatalytic

214   process in which there is no additional generation or consumption of protons beyond that

215   described in Equation (4). Na^+ is also included in the model, along with HCO_3^- as a

216   representative buffer. It was assumed that $S_2O_4^{2-}$, H_2O, SO_3^{2-}, HS^-, SO_4^{2-}, H^+, Na^+, and HCO_3^-

217   could be modeled as total components (Benjamin, 2014) in order to include equilibrium reactions

218   with secondary species dictated by the laws of mass action. This approach allows for a more

219   accurate calculation of proton activity. The model includes the secondary species and

220   corresponding mass action laws shown in Table 2, which are taken from the EQ3/6 database

221   (Wolery, 1992). As mentioned in Section I, sulfur possesses many oxidation states and

222   intermediate species that can form in aqueous solutions. Rather than include all potential

10

223   secondary species, we focus on well-established secondary species that form in the presence of

224   the reaction products in Equation 3 and whose equilibrium constants are readily available in the

225   EQ3/6 thermodynamic database. Activity coefficients were calculated in each time step using the

226   Debye-Hückel equation.

227   Equation (4) was coupled to Equation (2) in PFLOTRAN (Lichtner et al., 2017a,b) using

228   its "reaction-sandbox" interface (Hammond, 2015). A model calibration procedure was used to

229   simultaneously match the observed $S_2O_4^{2-}$ concentrations and pH trends at all three starting

230   dithionite concentrations in both the HCO_3^- and EDTA/OH^- buffered experiments. The

231   adjustable parameters were k and $\propto$. Additionally, because the reactions that occurred during the

232   early re-equilibration phase were very complex and too rapid to be quantified from the limited

233   number of samples that could be obtained from the sealed sacrificial reactors, the early dithionite

234   concentrations and pH values were treated as adjustable parameters that effectively match the

235   early observations very well. The model does not account for the early rapid degradation of

236   dithionite, which clearly gives rise to additional species in solution that alter buffering capacity.

237   The primary consideration was to accurately match the observed pH trends so that the pH

238   dependence of the dithionite degradation rate could be properly described via the fitted $\propto$

239   parameter. Finally, an additional parameter needed to match the observed pH trends was the

240   effective buffering capacity of the solutions, which was incorporated into the model as an

241   equivalent concentration of initial bicarbonate ($[HCO_3^-]_{eff}$) for each set of experiments.

242   Although the inclusion of an adjustable effective buffering capacity is a gross simplification of

243   potentially complex equilibrium reactions involving H^+, it is consistent with treating the initial

244   dithionite concentrations and pH as adjustable parameters, as these are all measures taken to

245   compensate for a lack of information available to explicitly account for early reaction processes,
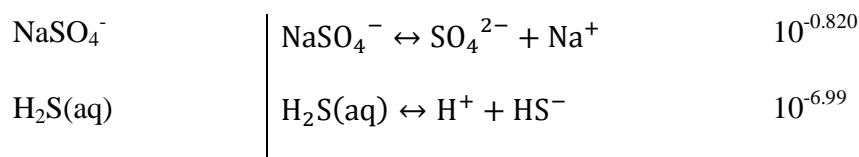
11

246   and in the case of the EDTA/OH- buffered experiments, also the inability to explicitly account

247   for the complexity of the added buffer. For the purposes of this study, the use of an adjustable

248   buffering capacity allowed for more accurate prediction of pH trends, which is required for the

249   parameterization of a pH dependent kinetic rate law. Calibration was achieved using the open-

250   source code MADS (Vesselinov and Harp, 2012). The model parameters were calibrated using

251   inverse analysis (utilizing Levenberg-Marquardt optimization) to reproduce the experimental

252   observations as defined in the MADS problem setup. For a more detailed description of the

253   PFLOTRAN-MADS calibration procedure, please refer to Appendix B.

254

255   Table 2. Secondary species with corresponding mass action laws and equilibrium constants (K)

256   used in the numerical model.

257

Secondary species	Mass action law	K
OH^-	$OH^- + H^+ \leftrightarrow H_2O$	$10^{14.0}$
CO_3^{2-}	$CO_3^{2-} + H^+ \leftrightarrow HCO_3^-$	$10^{10.3}$
$CO_2(aq)$	$CO_2(aq) + H_2O \leftrightarrow H^+ + HCO_3^-$	$10^{-6.34}$
HSO_3^-	$HSO_3^- \leftrightarrow H^+ + SO3^{2-}$	$10^{-7.21}$
$H_2SO_3(aq)$	$H_2SO_3(aq) \leftrightarrow 2H^+ + SO3^{2-}$	$10^{-9.21}$
HSO_4^-	$HSO_4^- \leftrightarrow H^+ + SO_4^{2-}$	$10^{-1.98}$
$H_2SO_4(aq)$	$H_2SO_4(aq) \leftrightarrow 2H^+ + SO_4^{2-}$	$10^{1.02}$
$NaCO_3^-$	$NaCO_3^- + H^+ \leftrightarrow HCO_3^- + Na^+$	$10^{9.81}$
$NaHCO_3(aq)$	$NaHCO_3(aq) \leftrightarrow HCO_3^- + Na^+$	$10^{-0.154}$
$NaOH(aq)$	$NaOH(aq) + H^+ \leftrightarrow H_2O + Na^+$	$10^{14.8}$

|		
$NaSO_4^-$	$NaSO_4^- \leftrightarrow SO_4^{2-} + Na^+$	$10^{-0.820}$
$H_2S(aq)$	$H_2S(aq) \leftrightarrow H^+ + HS^-$	$10^{-6.99}$

258

III. Results

III.A. Dithionite concentrations through time

Concentrations of dithionite, its hydrolysis products, and pH of the solutions determined during the experiments are reported figures 1-3. Figure 1 shows the decomposition of dithionite through time. The first measurement was taken 1 day after solutions were prepared. At this stage, determined concentrations of dithionite represented only a fraction of dithionite initially placed in the solution. This fraction systematically decreases with decreasing pH. For example, for HCO_3^- buffered solutions (pH=7.5 to 7.1), recovery of dithionite after 1 day was 26 to 30% of the initial concentrations (Fig. 1a). Conversely, in the EDTA/OH$^-$ buffered solutions having pH=9.1-9.7, this value ranged from 68 to 78% (Fig. 1b). It is likely that during the first days after solution preparation dithionite undergoes complex re-equilibration with its hydrolysis products: the first 3 samples taken demonstrated a relative increase of dithionite concentrations with respect to concentrations determined during day 1. The induction period and subsequent rapid autocatalytic reactions during the first few minutes of $S_2O_4^{2-}$ addition to aqueous solution have been the subject of intense study, but the current methods did not permit sampling at such frequent time intervals (Rinker et al., 1965; Burlamacchi et al., 1969; Wayman and Lem, 1970). The current study suggests that dithionite continues a rapid equilibration process over the time scale of a day or so, after which the dithionite undergoes a slow irreversible degradation until all the dithionite disappears (30+ days). Once the dithionite is gone, the reaction products presumably continue to interact with each other until a final geochemical and redox equilibrium

13

279   is reached. The unbuffered solutions experienced rapid loss of dithionite. Although the 0.1 M

280   solution persisted for 2-3 weeks, the 0.05 M and 0.025 M solutions had no measureable

281   dithionite after the first day (Fig. 1c). Because of the rapid loss of dithionite in the unbuffered

282   solutions, it would be impractical to consider an unbuffered dithionite deployment, so the

283   remainder of this paper focuses on the behavior of dithionite in the buffered solutions. For the

284   solutions buffered in HCO_3^-, dithionite disappeared after 29 days in the 0.1 M solution, whereas

285   the disappearance was 55 and 78 days in the 0.05 M and 0.025 M solutions, respectively (Fig.

286   1a). Similarly, the solutions buffered with EDTA/OH^- experienced more rapid loss for the 0.1 M

287   solution than the 0.05 and 0.025 M solutions. However, dithionite persisted much longer in all of

288   the EDTA/OH^- buffered solutions as compared to the HCO_3^- buffered solutions, lasting until 105

289   days in the 0.1 M solution, and remaining present until the end of the experiment (105 days; Fig.

290   1b) in the 0.05 and 0.025 M solutions.
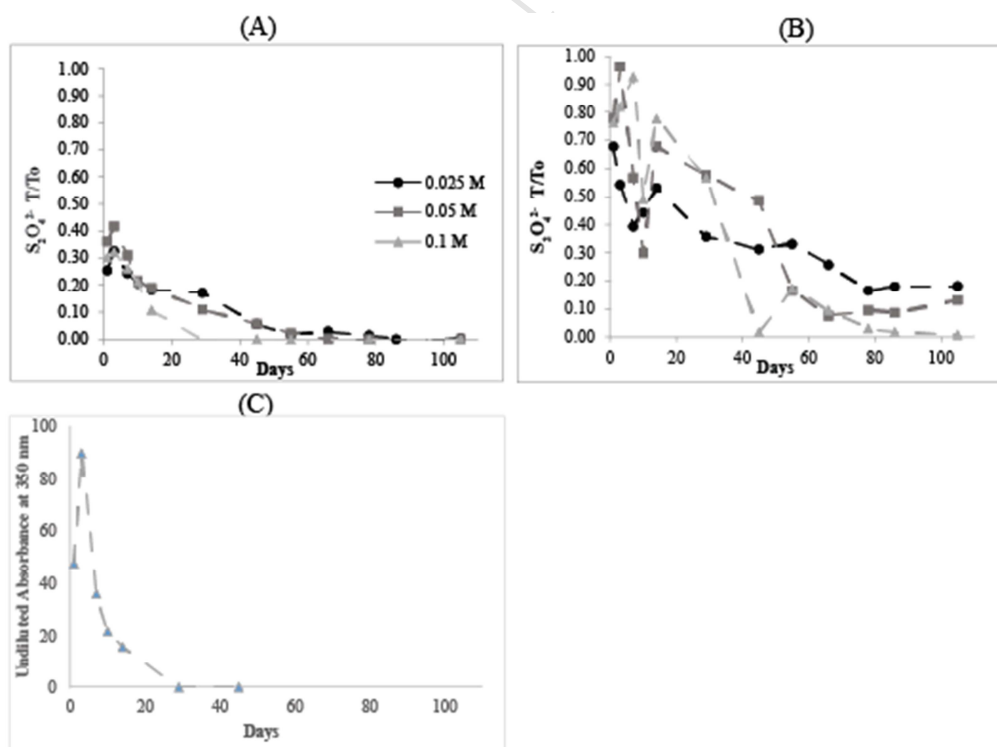
291

292 Figure 1: Dithionite decomposition through time in (A) HCO_3^-, (B) EDTA/OH⁻, and (C)

293 unbuffered solutions. A and B show the fraction of dithionite remaining relative to starting

294 concentrations. Absorbances are reported for the unbuffered solutions (C) as no calibration was

295 possible owing to the rapid degradation. Data are also reported in Appendix A.1.

296 *III.B. Degradation Products of Dithionite through time*

297   The hydrolysis products determined in the experiments demonstrate distinctively different

298 behavior. Sulfite (SO_3^{2-}) and sulfide (HS⁻) are found in nearly equimolar concentrations in

299 effectively all sampled solutions (Fig. 2a-d; Appendix A.2, A.3). Both of these species do not

300 show a definitive variation with time. The large temporal variability of the concentrations of

301 SO_3^{2-} may be due, in part, to experimental errors. In order to prevent saturating the UV-detector,

302 a very small amount of sample (0.05 mL) was diluted substantially (1210 times). The accuracy

303 of the syringe is 0.01 mL, and thus the error with the SO_3^{2-} measurements may be as high as

304 20%. However, it is apparent that in all samples, the SO_3^{2-} concentrations experience an initial

305 increase similar to that of $S_2O_4^{2-}$. Sulfite in the HCO_3^- buffered samples then appears to plateau

306 before dropping off at around 50-60 days (Fig. 2a). Sulfite in the EDTA/OH⁻ buffered samples,

307 however, decreases around 30 days but then increase by the end of the experiment (Fig. 2b).

308 Sulfite accounts for between 2 and 12% of the total S in EDTA/OH⁻ buffered solutions and

309 between 3 and 20% in HCO_3^- buffered solutions

310   In HCO_3^- buffered solutions, the concentration of SO_4^{2-} decreases with time (Fig. 2e). In

311 the first 2 samples, SO_4^{2-} accounts for about 33% of total S, but by the completion of the

312 experiment accounts for between 5 and 20%. A similar pattern is seen with the 0.1 M sample in

313 EDTA/OH⁻ buffered solution, in which the percentage of SO_4^{2-} accounting for total S drops from

15

314   33% to 5 %. However, the 0.05 and 0.025 M solutions have relatively steady SO_4^{2-}

315   concentrations through time (Fig. 2f).
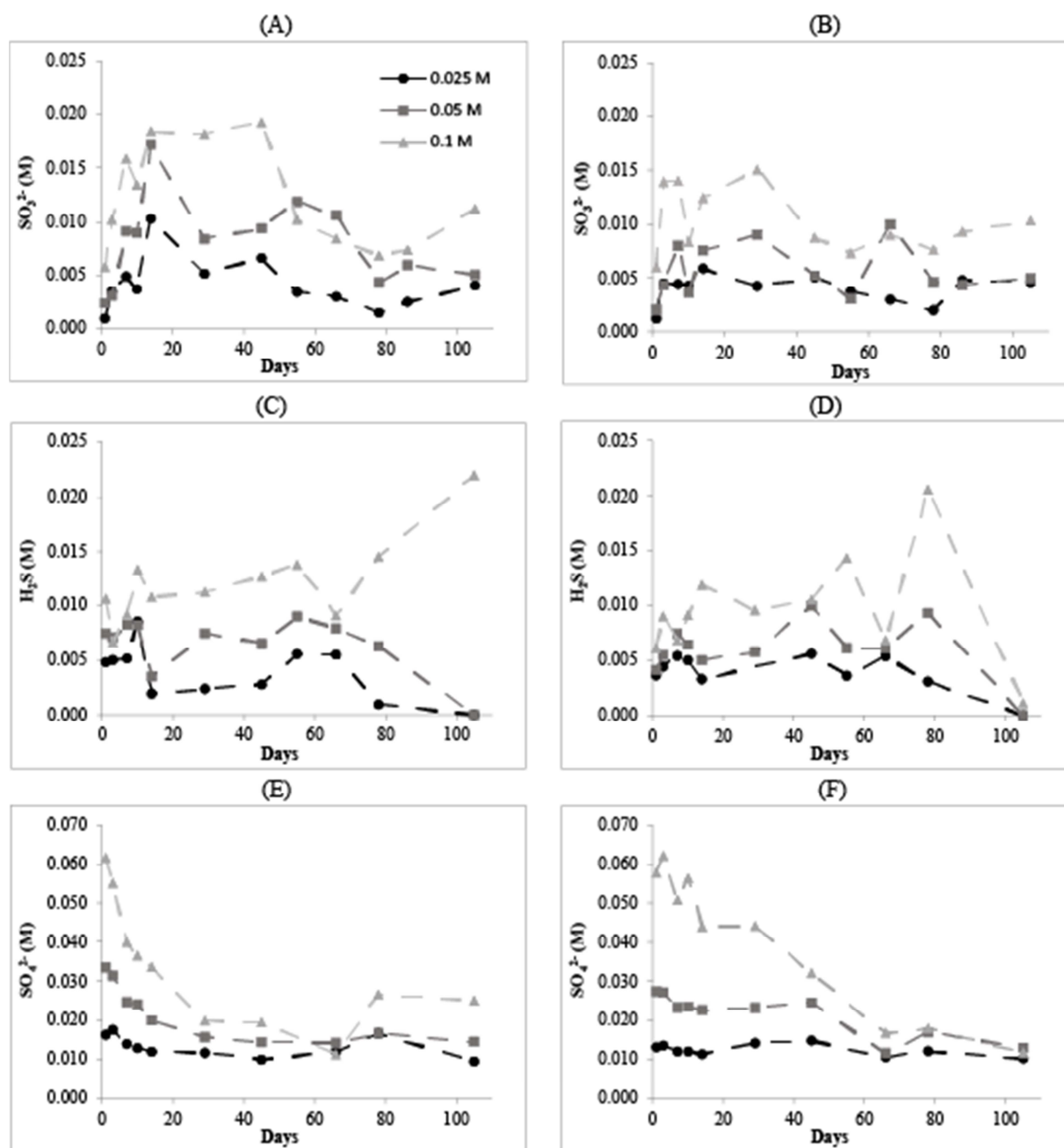
316

317   Figure 2: Concentrations of (A, B) SO_3^{2-}, (C, D) H_2S, and (E, F) SO_4^{2-} through time in (A, C, E)

318   HCO_3^- buffered and (B, D, F) EDTA/OH^- buffered solutions. Concentrations are also reported in

319   Appendix A.2, A.3.

16

320   In all samples, the pH decreases through time, and the decrease is more pronounced with

321 increasing concentrations for the HCO_3^- buffered and EDTA/OH⁻ solutions, whereas the pH of

322 the 0.1 M unbuffered solution is higher than either the 0.05 M or 0.025 M unbuffered solutions

323 (Fig. 3). More specifically, in the HCO_3^- buffered solutions, the pH drops from 7.5 to 7.3 in the

324 0.025 M solution, from 7.3 to 7.0 in the 0.05 M solution, and from 7.0 to 6.8 in the 0.1 M

325 solution (Fig. 3a). Similarly, in the EDTA/OH⁻ buffered solution, the pH drops from 9.7 to 9.6 in

326 the 0.025 M solution, from 9.5 to 9.2 M in the 0.05 M solution and from 9.1 to 7.9 in the 0.1 M

327 solution (Fig. 3b).
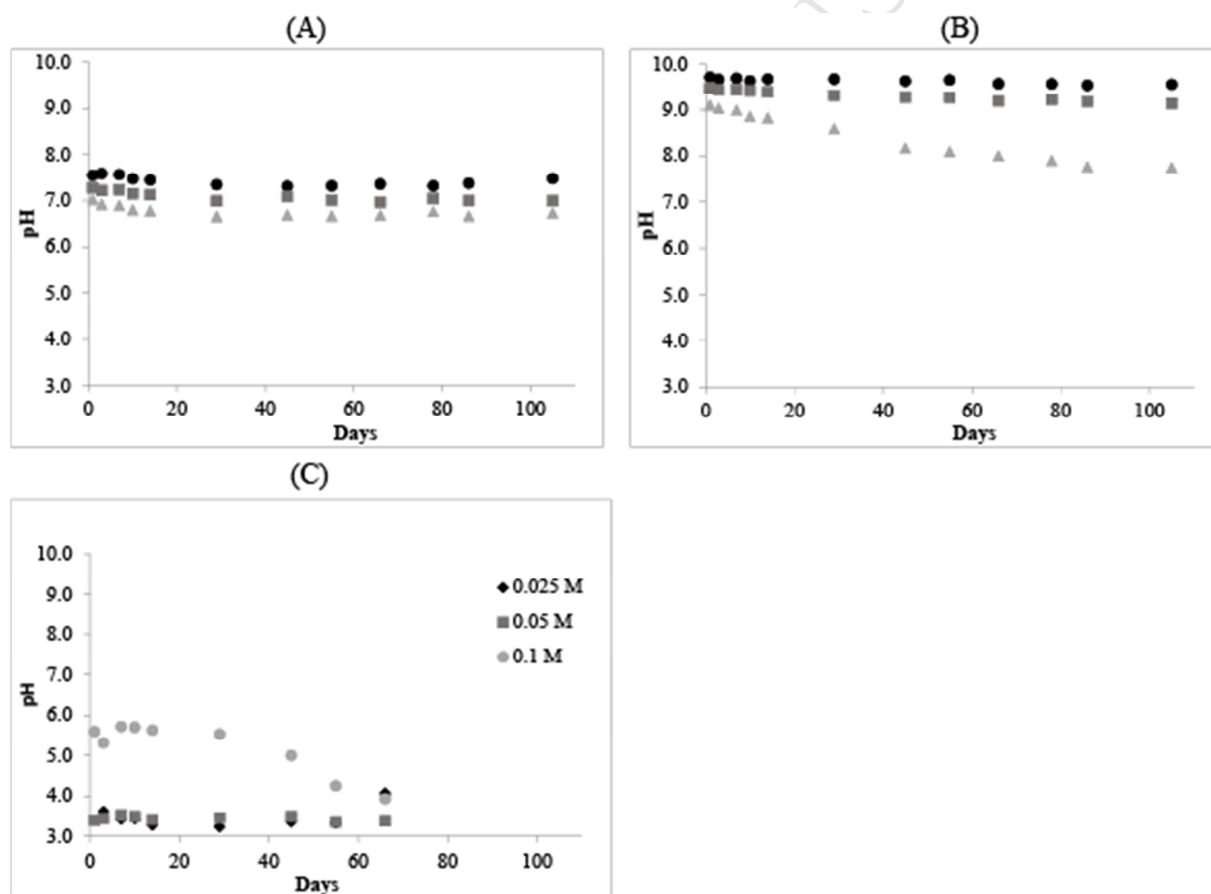
328

329 Figure 3: pH through time in (A) HCO_3^- buffered, (B) EDTA/OH⁻ buffered, and (C) unbuffered

330 solutions. pH values are also reported in Appendix A.2, A.3.

IV. Discussion

IV. A. Hydrolysis of dithionite

331

332

333 Faster degradation of dithionite at lower pH is consistent with previous studies (Lister and

334 Garvie, 1959; Kilroy, 1980; Ammonette et al., 1994). However, accounting for all previously

335 reported major degradation products (i.e., SO_3^{2-}, $S_2O_3^{2-}$) (Lister and Garvie, 1959; Münchow and

336 Steudel, 1994; de Carvalho and Schwedt, 2001, 2005) in these experiments demonstrates that a

337 substantial proportion of sulfur cannot be accounted for in near-neutral solutions (pH=7.5 to 7.1).

338 The sum of the S species determined in these experiments was only 68 to 78% of the initial total

339 sulfur concentrations right at the first day of the experiments and demonstrated continuous

340 decrease with time (Fig. 4a). At alkaline conditions (pH = 9.0 - 9.7), measured sulfur species

341 accounted for almost 100% of initial total sulfur concentrations during the first 30 days of the

342 experiment (Fig. 4b). Based on the analytical techniques used, the experiments were unable to

343 account for all S species, in particular, zero-valent sulfur, some of the polythionate species,

344 and/or elemental sulfur involved in polysulfane chains. The initial unbuffered solutions became

345 milky white, suggesting the formation of colloidal S at low pH (~4), and other experiments have

346 also suggested the formation of elemental S during the decomposition of dithionite (Rinker et al.,

347 1965; Wayman and Lem, 1970; de Carvalho and Schwedt, 2001). de Carvalho and Schwedt

348 (2001) note the disappearance of elemental sulfur within 24 hours, which is consistent with our

349 observations of the unbuffered solutions.

350

351
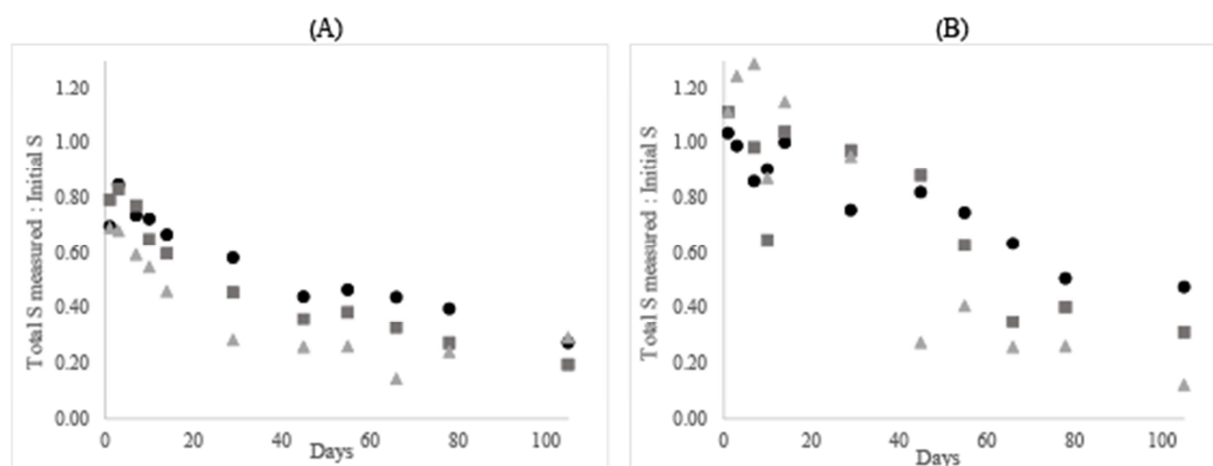
Figure 4: Ratio of measured S relative to the starting concentration in (A) HCO_3^- buffered and

(B) EDTA/OH- buffered solutions.

In addition to elemental S, which appeared to be important only at very low pH

(unbuffered solutions), dithionite decomposition may produce polythionates. The decomposition

of polythionates produces sulfate, elemental sulfur, and hydrogen ions and is thus consistent with

the analytically measured products (Meyer and Ospina, 1982; Takano, 1987; Takano et al.,

1994a; Druschel et al., 2003a,b). Therefore, we hypothesize that in these solutions formation of

polythionate $S_4O_6^{2-}$ has occurred, and that the hydrolysis reaction of dithionite can be expressed

as follows:

$$4\ S_2O_4^{2-} + H_2O \rightarrow HS^- + SO_3^{2-} + 2\ SO_4^{2-} + S_4O_6^{2-} + H^+ \qquad (3)$$

This reaction progresses to a lesser extent as pH increases, consistent with polythionates having

greater stability at low pH and undergoing decomposition at higher pH (Meyer and Ospina,

1982; Druschel et al., 2003a,b). Reaction 2 therefore is a proxy for the more rapid process of

dithionite degradation observed at near-neutral pH (HCO_3^- buffered solutions). The

stoichiometry of reaction 2 accounts for the initial production of protons and polythionates (i.e.,

19

367   unaccounted for sulfur species) observed in HCO_3^- buffered experiments at each dithionite

368   concentration. Because we were not able to directly measure the various polythionates and

369   elemental sulfur, it is possible that the $S_4O_6^{2-}$ term represents the summation of other

370   unaccounted for S species. Nevertheless, at higher pH values (EDTA/OH^- buffered solutions)

371   and on longer time scales, this term becomes less important and the reaction is better represented

372   as:

373         $$3\ S_2O_4^{2-} + 3\ H_2O \rightarrow 2HS^- + SO_3^{2-} + 3\ SO_4^{2-} + 4\ H^+ \qquad (4)$$

374   .
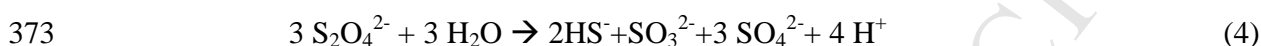
375   *IV. B. Kinetics of dithionite decomposition*

376

377   Equation (5) shows the parameterized kinetic rate law:

378         $$\frac{dC_i}{dt} = S_i 10^{-4.81}\{H^+\}^{0.24}\{S_2O_4^{2-}\}, \qquad (5)$$

379   where $\frac{dC_i}{dt}$ has units of mol L^{-1} s^{-1}. Results of model calibration are shown in Figures 5 and 6, and

380   additional calibrated model parameters for the two sets of experiments are shown in Table 3

381   (note that although the initial pH and initial $[S_2O_4^{2-}]$ in each experiment were technically

382   "calibrated", the model effectively just matched these parameters to their observed values after

383   the initial rapid equilibration period) . In general, the kinetic rate model with equilibrium

384   speciation was capable of fitting the $[S_2O_4^{2-}]$ and pH data simultaneously for all initial $S_2O_4^{2-}$

385   concentrations in both the HCO_3^- buffered and EDTA/OH^- buffered experiments. $[HCO_3^-]_{eff}$ for

386   the HCO_3^- buffered solutions (0.329 M) was found to be higher than the 0.1 M HCO_3^- used,

387   which is most likely due to the early rapid generation of reaction products that have buffering

388   capacity (e.g. $H_2S_4O_6(aq)$, $HS_4O_6^-$) not considered in the model. The high calibrated value of

389    $[HCO_3^-]_{eff}$ for the EDTA/OH$^-$ buffered experiments (0.570 M) was likely due to the complex

390   buffers used in stock buffer solution.

391

392   Table 3. Additional calibrated parameters used in the numerical model.

393

Parameter	Units	pH 8.3	pH 10
pH_i, 0.1 M $S_2O_4^{-2}$	-	7.15	9.14
pH_i, 0.05 M $S_2O_4^{-2}$	-	7.43	9.55
pH_i, 0.025 M $S_2O_4^{-2}$	-	7.71	9.81
$[S_2O_4^{-2}]_i$, 0.1 M $S_2O_4^{-2}$	M	0.0391	0.0897
$[S_2O_4^{-2}]_i$, 0.05 M $S_2O_4^{-2}$	M	0.0180	0.0397
$[S_2O_4^{-2}]_i$, 0.025 M $S_2O_4^{-2}$	M	0.00897	0.0151
$[HCO_3^-]_{eff}$	M	0.329	0.570

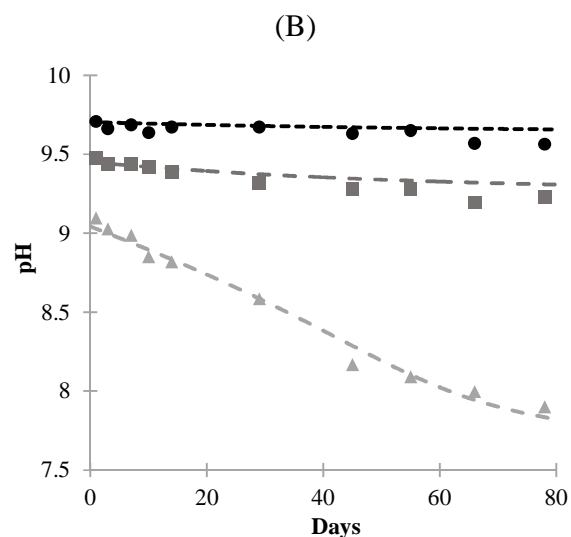(A)   (B)
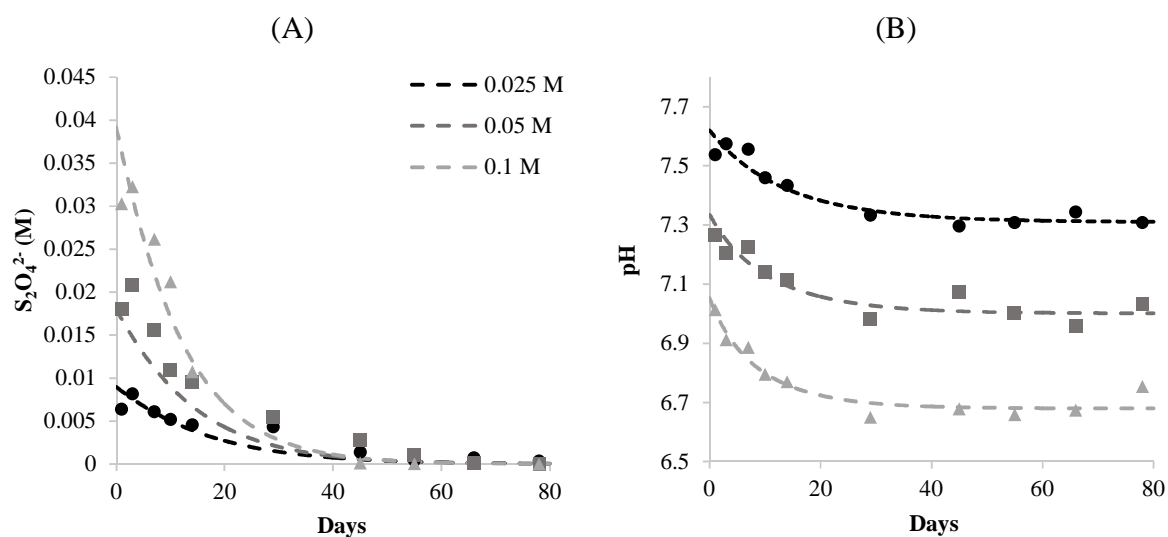
394

395   Figure 5. Simulation of experiments conducted in the HCO_3^- buffered solution. Panel (A) shows

396   the dithionite concentration, and Panel (B) shows pH. The figure compares calibrated model

397   curves (dashed lines) and experimental data (points) for the different concentrations of dithionite

398   used in these experiments.

399

400

(A)

401

(B)
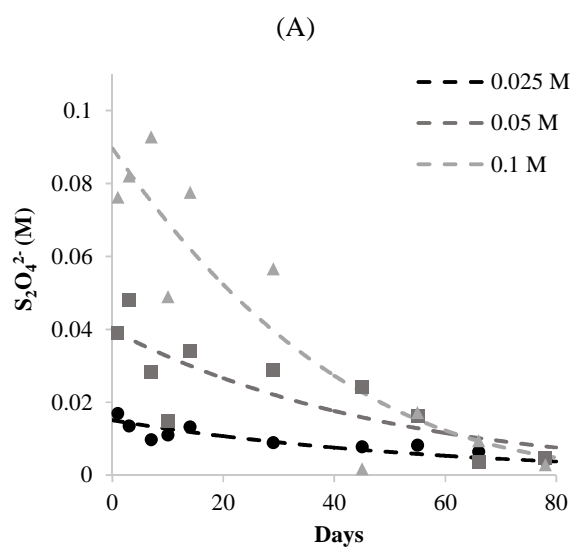
402   Figure 6. Simulation of experiments conducted in the EDTA/OH⁻ buffered solution. Panel (A)

403   shows the dithionite concentration, and Panel (B) shows pH. The figure compares calibrated

22

404   model curves (dashed lines) and experimental data (points) for the different concentrations of

405   dithionite used in these experiments. The fitted model parameters, k and $\propto$ of equation (4), are

406   identical for the model curves of Figures 5 and 6.

407   Equation (5) was used to estimate half-lives of each experiment by treating

408    $10^{-4.81}\{H^+\}_i^{0.24}$ as a pseudo first order rate constant, where $\{H^+\}_i$ is the initial proton activity

409   calculated using the calibrated value of pH_i, and normalizing by the stoichiometric coefficient of

410    $S_2O_4^{2-}$ in Equation (4). The estimated half-lives for the HCO_3^- buffered experiments were 9.06,

411   10.6, and 12.4 days for the 0.1, 0.05, and 0.025 M dithionite concentrations, respectively,

412   resulting in a mean half-life of 10.7 days. The estimated half-lives for the EDTA/OH$^-$ buffered

413   experiments were 27.2, 34.2, and 39.5 days for 0.1 M, 0.05 M, and 0.025 M dithionite

414   concentrations respectively, resulting in a mean half-life of 33.6 days. The mean values represent

415   single best estimates that consider all initial starting concentrations for a given pH while also

416   assuming that the half-life varies with pH but not dithionite concentration (pseudo first-

417   order). The longer half-life reported at the higher pH in the present study relative to the half-lives

418   reported by Amonette et al. (1994) at a similar pH is most likely the result of preventing any

419   gases from either entering or leaving the glass-sealed ampoules in the current study. It is well

420   known that oxygen reacts rapidly with dithionite (Rinker et al., 1960; Creutz and Sutin, 1974),

421   and care was taken in both studies to minimize or eliminate oxygen, but the present study also

422   prevented the egress of gasses from the reaction vessels. Amonette et al. (1994) do not mention

423   any measures taken to prevent H_2S egress (which can occur through many types of vessel caps or

424   stoppers), and we hypothesize that keeping the H_2S in our reaction vessels slowed the

425   degradation of dithionite because it maintained a higher concentration of the degradation

426   product(s) HS^-/S^{2-} in solution.

23

427   Although the rate law (equation 5) can effectively predict the post-rapid-hydrolysis

428   degradation rate as a function of pH, several lines of evidence suggest that assuming reaction (4)

429   accounts for all dithionite degradation and using only the limited assemblage of species and

430   reactions in Table 2 greatly oversimplifies the system. The fact that the pH trends in the

431   experiments can only be matched if the initial effective pH buffering of the system (the first ~ 3

432   days) is treated as an adjustable parameter is one such line of evidence. Also, as $S_2O_4^{2-}$

433   concentrations decrease with time, the concentrations of reaction (4) products SO_4^{2-}, SO_3^{2-} and

434   HS^- measured in the experiments either decreased or stayed relatively constant. This is contrary

435   to simulation results. These species are reaction products in reaction (3), so the model predicted

436   that their concentration would increase proportionally to the amount of dithionite that is

437   degraded. Instead, it is the concentration(s) of the unaccounted for reduced S species, which are

438   not considered in the model, that consistently increase with time. These observations suggest

439   that (1) there are unaccounted-for reaction products that are involved in hydrolysis and acid-base

440   reactions that are not considered by the model, and (2) the sulfur chemistry evolves in a complex

441   manner as a result of interactions between reduced and oxidized sulfur reaction products that are

442   not thermodynamically compatible.

443   *IV. C. Implications for Environmental Remediation*

444   As a strong reducing agent, dithionite has the potential to be a useful chemical for

445   environmental remediation of oxic contaminants, such as Cr(VI). However, its high reactivity

446   makes it challenging to deploy in the field, and even if oxygen is eliminated from solution before

447   addition, dithionite degradation still occurs at a significant rate. The results of this study suggest

448   that in order to develop a complete mechanistic model of dithionite degradation, simultaneous

449   determination of every S species on the time scale of minutes would be required. However, we

450 reasoned that the early-time degradation behavior of dithionite, other than the fraction of

451 dithionite remaining, is not of practical importance because this rapid degradation will occur

452 almost immediately upon dissolving dithionite. Thus, we focused on the development of a semi-

453 mechanistic, semi-empirical rate law describing anoxic aqueous decomposition of dithionite as a

454 function of pH *after* the initial rapid degradation/equilibration process. Although we did not

455 address dithionite decomposition in the presence of oxygen or aquifer sediments, knowledge of

456 anaerobic decomposition rates should prove valuable for such follow-on studies because anoxic

457 decomposition will always be superimposed on oxic decomposition. From a practical

458 standpoint, the anoxic conditions of this study are relevant for estimating how far into an aquifer

459 dithionite can be "pushed" from an injection well. Assuming dithionite reacts rapidly with any

460 dissolved oxygen and oxidized sediments that are present in the aquifer (e.g., ferric and

461 manganese oxides), these oxic reactants will eventually be consumed in the vicinity of an

462 injection well, and if dithionite is continuously injected, the distance that it can ultimately be

463 pushed into an aquifer will be dictated by its anaerobic decomposition rate in the presence of

464 aqueous phase reaction products.

465 It was determined that ~70% of dithionite hydrolyzes almost immediately in a HCO_3^-

466 buffered anoxic system and about 20% hydrolyzes immediately in an anoxic solution buffered to

467 pH ~9.5. However, in both cases, the decomposition of the remaining dithionite is much slower,

468 with dithionite concentrations remaining measurable for over 50 and 100 days, respectively. This

469 observation has important implications for field deployments, namely that loss of dithionite due

470 to anoxic decomposition occurs more slowly than previously thought. The half-lives reported

471 here are 2 times longer than those reported by Ammonette et al. (1994) for comparable pHs and

472 dithionite concentrations, which we attribute to keeping volatile reaction products, such as H_2S

473   gas, from escaping from the reactors. Such volatile reaction products should also remain in

474   solution in confined aquifers, particularly when an overpressure is imposed to inject a dithionite

475   solution at a reasonable rate. This implies that in an ideal system of radial flow near an injection

476   well (penetration distance into aquifer proportional to square root of time), dithionite can be

477   effectively injected $\sqrt{2}$ times further into an aquifer than previously thought for a given injection

478   flow rate. Consequently, the spacing of injection wells for establishing an in-situ barrier can be

479   increased, which can translate to significant cost savings, particularly in deep, contaminated

480   aquifers, such as those in Los Alamos.

481

486

487   **References**

488   Amonette, J. E.; Szecsody, J. E.; Schaef, H. T.; Templeton, J. C.; Gorby, Y. A.; Fruchter, J. S.,
489   1994. Abiotic reduction of aquifer materials by dithionite: a promising in-situ
490   remediation technology. (No. PNL-SA_24505; CONF-941124022). Pacific Northwest
491   Lab., Richland, WA (United States).
492   Benjamin, M. M., 2014 Water chemistry; Waveland Press: Illinois.
493   Boparai, H. K.; Comfort, S. D.; Shea, P. J.; Szecsody, J. E., 2008 Remediating explosive-
494   contaminated groundwater by in situ redox manipulation (ISRM) of aquifer sediments.
495   Chemosphere. 71 (5), 933-941.
496   Burlamacchi, L., Guarini, G., Tiezzi, E., 1969. Mechanism of decomposition of sodium
497   dithionite in aqueous solution. Trans. of the Faraday Soc. 65, 496-502.
498   Burton, E. D.; Bush, R. T.; Johnston, S. G.; Sullivan, L. A.; Keene, A. F., 2011. Sulfur
499   biogeochemical cycling and novel Fe-S mineralization pathways in a tidally re-flooded
500   wetland. Geochim. Cosmochim. Acta. 75 (12), 3434-3451.
501   Casas, A. S.; Armienta, M. A.; Ramos, S., 2016 Sulfur speciation with high performance liquid
502   chromatography as a tool for El Chichón volcano, crater lake monitoring. J. South Am.
503   Earth Sci. 72, 241-249.

504 Couture, R.. M.; Fischer, R.; Van Cappellen, P.; Gobeil, C., 2016. Non-steady state diagenesis of
505   organic and inorganic sulfur in lake sediments. Geochim. Cosmochim Acta. 194, 15-33.
506 Creutz, C.; Sutin, N., 1974. Kinetics of the reactions of sodium dithionite with dioxygen and
507   hydrogen peroxide. Inorg. Chem. 13 (8), 2041–2043.
508 Danehy, J. P.; Zubritsky, C. W., 1974. Iodometric method for the determination of dithionite,
509   bisulfite, and thiosulfate in the presence of each other and its use in following the
510   decomposition of aqueous solutions of sodium dithionite. Anal. chem. 46 (3), 391-395.
511 de Carvalho, L. M.; Schwedt, G., 2001. Polarographic determination of dithionite and its
512   decomposition products: kinetic aspects, stabilizers, and analytical application. Anal.
513   Chim. Acta. 436 (2) 293-300.
514 de Carvalho, L. M.; Schwedt, G., 2005. Sulfur speciation by capillary zone electrophoresis
515   Determination of dithionite and its decomposition products sulfite, sulfate and thiosulfate
516   in commercial bleaching agents. J. Chromatogr. A. 1099 (1), 185-190.
517 Druschel, G. K.; Hamers, R. J.; Banfield, J. F., 2003a. Kinetics and mechanism of polythionate
518   oxidation to sulfate at low pH by O2 and Fe3+. Geochim. Cosmochim. Acta. 67 (23),
519   4457-4469.
520 Druschel, G. K.; Hamers, R. J.; Luther, G. W.; Banfield, J. F., 2003b. Kinetics and mechanism of
521   trithionate and tetrathionate oxidation at low pH by hydroxyl radicals. Aquat. Geochem.
522   9 (2), 145-164.
523 Fruchter, J. S.; Cole, C. R.; Williams, M. D.; Vermeul, V. R.; Amonette, J. E.; Szecsody, J. E.;
524   Istok, J. D.; Humphrey, M. D., 1999. Creation of a subsurface permeable treatment zone
525   for aqueous chromate contamination using in situ redox manipulation. Groundwater
526   Monit. Rem. 20 (2), 66-77.
527 Hammond, G. E., 2015. PFLOTRAN: Recent Developments Facilitating Massively-Parallel
528   Reactive Biogeochemical Transport, in: AGU Fall Meeting, American Geophysical
529   Union Fall Meeting, 2015.
530 Holman, D. A.; Bennett, D. W., 1994. A multicomponent kinetics study of the anaerobic
531   decomposition of aqueous sodium dithionite. J. Phys. Chem. 98 (50), 13300-13307.
532 Istok, J. D.; Amonette, J. E.; Cole, C. R.; Fruchter, J. S.; Humphrey, M. D.; Szecsody, J. E.; Teel,
533   S. S.; Vermeul, V. R.; Williams, M. D.; Yabusaki, S. B., 1999. In situ redox manipulation
534   by dithionite injection: intermediate-scale laboratory experiments. Ground water. 37 (6),
535   884-889.
536 Kaasalainen, H.; Stefánsson, A., 2011a. Sulfur speciation in natural hydrothermal waters,
537   Iceland. Geochim. Cosmochim. Acta. 75 (10), 2777-2791.
538 Kaasalainen, H. Stefánsson, A., 2011b Chemical analysis of sulfur species in geothermal waters.
539   Talanta 85 (4), 1897-1903.
540 Kilroy, W. P., 1980. Anaerobic decomposition of sodium dithionite in alkaline solution. J. Inorg.
541   Nucl. Chem. 42 (7), 1071-1073.
542 Lem, W. J., Wayman, M., 1970. Decomposition of aqueous dithionite. Part I. Kinetics of
543   decomposition of aqueous sodium dithionite. Canadian Journal of Chemistry, 48(5): 776-
544   781.
545 Lichtner, P. C.; Hammond, G. E.; Lu, C.; Karra, S.; Bisht, G.; Andre, B.; Mills, R. T.; Kumar,
546   J.; Frederick, J. M., 2017a. PFLOTRAN User Manual;
547   http://www.documentation.pflotran.org.
548 Lichtner, P. C.; Hammond, G. E.; Lu, C.; Karra, S.; Bisht, G.; Andre, B.; Mills, R. T.; Kumar, J.;
549   Frederick, J. M., 2017b. PFLOTRAN Webpage; http://www.pflotran.org.

550 Lister, M. W.; Garvie, R. C., 1959. Sodium dithionite, decomposition in aqueous solution and in
551   the solid state. Can J. Chem. 37 (9), 1567-1574.
552 Ludwig, R. D.; Su, C.; Lee, T. R.; Wilkin, R. T.; Acree, S. D.; Ross, R. R.; Keeley, A., 2007. In
553   situ chemical reduction of Cr(VI) in groundwater using a combination of ferrous sulfate
554   and sodium dithionite: A field investigation. Environ. Sci. Technol. 41 (15), 5299-5305.
555 Luther, G. W.; Church, T. M., 1998. Seasonal cycling of sulfur and iron in porewaters of a
556   Delaware salt marsh. Marine Chemistry 23 (3-4), 295-309.
557 Meyer, B.; Ospina, M., 1982. Raman spectrometric study of the thermal decomposition of
558   aqueous tri- and tetrathionate. Phosphorus Sulfur Relat. Elem. 14 (1), 23-36.
559 Migdisov, A. A.; Bychkov, A. Y., 1998. The behavior of metals and sulphur during the
560   formation of hydrothermal mercury—antimony—arsenic mineralization, Uzon caldera,
561   Kamchatka, Russia. J. Volcanol. Geotherm. Res. 4, 153-171.
562 Münchow, V.; Steudel, R., 1994. The decomposition of aqueous dithionite and its reactions with
563   polythionates SnO62- (n=3-5) studied by ion-pair chromatography. Z. Anorg. Allg.
564   Chem. 620 (1), 121-126.
565 Nzengung, V. A., Castillo, R. M., Gates, W. P., Mills, G. L., 2001. Abiotic transformation of
566   perchloroethylene in homogeneous dithionite solution and in suspensions of dithionite-
567   treated clay minerals. Environ. Sci. Technol. 35 (11), 2244-2251.
568 Rinker, R. G.; Gordon, T. P.; Mason, D. M.; Sakaida, R. R.; Corcoran. W. H., 1960. Kinetics and
569   mechanism of the air oxidation of the dithionite ion (S2O4=) in aqueous solution. J. Phys.
570   Chem. 64 (5), 573–581.
571 Rinker, R. G.; Lynn, S.; Mason, D. M.; Corcoran, W. H., 1965. Kinetics and mechanism of
572   thermal decomposition of sodium dithionite in aqueous solution. Ind. Eng. Chem.
573   Fundam. 4 (3), 282-288.
574 Spencer, M. S., 1967. Chemistry of sodium dithionite. Part 1.—Kinetics of decomposition in
575   aqueous bisulphite solutions. Transactions of the Faraday Society, 63: 2510-2515.
576 Szecsody, J. E., Fruchter, J. S., Williams, m. D., Vermeul, V. R., Sklarew, D., 2004. In situ
577   chemical reduction of aquifer sediments: enhancement of reactive iron phases and TCE
578   dechlorination. Environ. Sci. Technol. 38 (17), 4656-4663.
579 Szekeres, L., 1974. Analytical chemistry of the sulfur acids. Talanta. 21 (1), 1-44.
580 Takano, B., 1987. Correlation of volcanic activity with sulfur oxyanion speciation in a crater
581   lake. Science. 235, 1633-1636.
582 Takano, B.; Watanuki, K., 1990. Monitoring of volcanic eruptions at Yugama crater lake by
583   aqueous sulfur oxyanions. J. Volcanol. Geotherm. Res. 40 (1), 71-87.
584 Takano, B.; Ohsawa, S.; Glover, R. B., 1994a. Surveillance of Ruapehu Crater Lake, New
585   Zealand, by aqueous polythionates. J. Volcanol. Geotherm. Res. 60 (1), 29-57.
586 Takano, B.; Saitoh, H.; Takano, E., 1994b. Geochemical implications of subaqueous molten
587   sulfur at Yugama crater lake, Kusatsu-Shirane volcano, Japan. Geochem. J. 28 (3), 199-
588   216.
589 Vesselinov, V.; Harp, D., 2012. June. Model analysis and decision support (MADS) for comple
590   physics models. In XIX International conference on water resources-CMWR.
591 Wayman, M.; Lem, W. J., 1970. Decomposition of aqueous dithionite. Part II. A reaction
592   mechanism for the decomposition of aqueous sodium dithionite. Can J. Chem. 48 (5),
593   782-787.
594 Williamson, M. A.; Rimstidt, J. D., 1992. Correlation between structure and thermodynamic
595   properties of aqueous sulfur species. Geochim. Cosmochim. Acta. 56 (11), 3867-3880.

596 Wolery, T.J., 1992. EQ3/6: A software package for geochemical modeling of aqueous systems:
597   package overview and installation guide (version 7.0) (pp. 1-65). Livermore, CA:
598   Lawrence Livermore National Laboratory.
599 Xie, Y.; Cwiertny, D. M., 2010. Use of dithionite to extend the reactive lifetime of nanoscale
600   zero-valent iron treatment systems. Environ. Sci. Technol. 44 (22), 8649-8655.
601 Xu, Y.; Schoonen, M. A. A.; Nordstrom, D. K.; Cunningham, K. M.; Ball, J. W., 1998. Sulfur
602   geochemistry of hydrothermal waters in Yellowstone National Park: I. The origin of
603   thiosulfate in hot spring waters. Geochim. Cosmochim. Acta. 62 (23), 3729-3743.

Highlights: Long-term stability of dithionite in alkaline anaerobic aqueous solution

1. Sodium dithionite concentrations in alkaline aqueous solutions were measured by UV-vis spectrometry for up to 105 days.
2. Analysis of degradation products revealed that sulfite, hydrogen sulfide, sulfate, and polythionates are present.
3. The closed system created in this study ensured no loss of hydrogen sulfide, which slowed the loss of dithionite.
4. The kinetic rate law developed yields a half-life of 10.7 days at near-neutral pH and 33.6 days at alkaline pH.